Author/s:
Nyman, P;Box, WAC;Stout, JC;Sheridan, GJ;Keesstra, SD;Lane, PNJ;Langhans, C

Title:
Debris-flow-dominated sediment transport through a channel network after wildfire

Date:
2020-04-01

Citation:
Nyman, P., Box, W. A. C., Stout, J. C., Sheridan, G. J., Keesstra, S. D., Lane, P. N. J. & Langhans, C. (2020). Debris-flow-dominated sediment transport through a channel network after wildfire. Earth Surface Processes and Landforms, 45 (5), pp.1155-1167. https://doi.org/10.1002/esp.4785.

Persistent Link:
https://hdl.handle.net/11343/275399

Debris-flow dominated sediment transport through a channel network after wildfire

Short title: Debris-flow dominated sediment transport through a channel network

Petter Nyman[1], Walter AC Box[1], Justin C Stout[3,5], Gary J Sheridan[1], Saskia D Keesstra[4], Patrick NJ Lane[1], Christoph Langhans[1,2]

[1] School of Ecosystems and Forest Sciences, The University of Melbourne, Parkville, Victoria 3010, Australia

[2] Netherlands Environmental Assessment Agency (PBL), 2594 AV, The Hague, The Netherlands

[3] Griffith Centre for Coastal Management, Griffith University, Queensland 4215, Australia

[4] Soil Physics and Land Management Group, Wageningen University, 6708PB Wageningen, The Netherlands

[5] School of Geography, The University of Melbourne, Parkville, Victoria 3010, Australia

Submitted to *Earth Surface Processes and Landforms*

Corresponding author:

Petter Nyman

School of Ecosystem and Forest Science,

The University of Melbourne,

Baldwin Spence Building (West)

Parkville, 3010 Victoria,

Australia

Phone: +61 408584676

Email: nymanp@unimelb.edu.au

Abstract

Field studies that investigate sediment transport between debris-flow producing headwaters and rivers are uncommon, particularly in forested settings, where debris flows are infrequent and opportunities for collecting data are limited. This study quantifies volume and composition of sediment deposited in the arterial channel network of a 14 km^2 catchment (Washington Creek) that connects small, burned and debris-flow producing headwaters (<1 km^2) with the Ovens River in SE Australia. We construct a sediment budget by combining new data on deposition with a sediment delivery model for post-fire debris flows. Data on deposits were plotted alongside the slope-area curve to examine links between processes, catchment morphometry, and geomorphic process domains. Results show that large deposits are concentrated in the proximity of three major channel junctions, which correspond with breaks in channel slope. Hyperconcentrated flows are more prominent towards the catchment outlet where the slope-area curve indicates a transition from debris flow to fluvial domains. This shift corresponds to a change in efficiency of the flow, determined from the ratio of median grain size to channel slope. Our sediment budget suggests a total sediment efflux from Washington Creek catchment of 61 x 10^3 m^3. There are similar contributions from hillslopes (43±14 x 10^3 m^3), 1-3rd stream order channel (35±12 x 10^3 m^3) and the arterial 4-5th stream order channel (31±17 x 10^3 m^3) to the total volume of erosion. Deposition (39±17 x 10^3 m^3) within the arterial channel was higher than erosion (31±17 x 10^3 m^3), which means a net sediment gain of about 8 x 10^3 m^3 in the arterial channel. The ratio of total deposition to total erosion was 0.56. For fines < 63 µm, this ratio was much larger (0.89), which means that fines are preferentially exported. This has important implications for suspended sediment and water quality in downstream rivers.

Key words: Debris flow, wildfire, sediment deposition, sediment budget, channel network

1. Introduction

Debris flows are often the dominant process by which sediment is transported from steep headwaters to channels because they access sediments stored as colluvium in drainage lines and zero-order hollows. (Benda & Dunne, 1997a; Gomi, Sidle & Richardson, 2002; Montgomery, 1999). During a debris flow, sediment accumulated in headwaters over long timescales (decades to centuries) can become a major and sudden sediment source to rivers and channels, with implications for fluvial habitats (Harris, Baxter & Davis, 2015; Montgomery & Buffington, 1998) and water quality (Dahm, Candelaria-Ley, Reale, Reale & Van Horn, 2015; Smith, Sheridan, Lane, Nyman & Haydon, 2011). Sediments generated from debris flows can be transported a long distance downstream (e.g. Lyon & O'Connor, 2008) or deposited in valley-bottom fans, gravel bars or narrow flood plains, remaining in storage for decades to millennia depending on fluvial reworking (Lancaster, 2008; Lancaster & Casebeer, 2007; Pierce, Meyer & Rittenour, 2011).

Wildfire increases the susceptibility of landscapes to debris flows (Meyer & Pierce, 2003; Wondzell & King, 2003). Debris flows associated with wildfires (i.e. post-fire debris flows) can trigger major sediment transport in post-orogenic landscapes where background erosion rates are very low (e.g. SE Australia; Nyman, et al., 2015; Smith, et al., 2012). There is a substantial body of literature on post-fire debris flows focused on hazards (Cannon, et al., 2010; Riley, Bendick, Hyde & Gabet, 2013), the prediction of where and when they will occur (Gartner, Cannon, Santi & Dewolfe, 2008; Staley, et al., 2018), and how much sediment they produce (DeLong, Youberg, DeLong & Murphy, 2018; Gartner, Cannon & Santi, 2014; Gartner, et al., 2008; Nyman, et al., 2015; Santi, deWolfe, Higgins, Cannon & Gartner, 2008). A growing body of research is focusing on the physical mechanisms that give rise to post-fire debris flows, and the development of process-based debris-flow models (Kean, McCoy, Tucker, Staley & Coe, 2013; McGuire, Rengers, Kean & Staley, 2017; Rengers, McGuire, Kean, Staley & Hobley, 2016). However, much of this work has focused on debris-flow processes within steep headwaters where channel slopes sit well within the debris-flow domain (typically > 20 degrees). Below these steep headwaters there are systematic changes in channel geometry (e.g. roughness, planform, slope and valley confinement) and flow properties (e.g. discharge, flow velocity, density), which means that mechanisms of erosion and deposition shift from a debris-flow dominated domain to one that is dominated by fluvial processes.

Erosion and deposition through drainage networks has large implications for how debris flows translate to impacts on downstream water resources (Bladon, Emelko, Silins & Stone, 2014; Murphy, McCleskey, Martin, Writer & Ebel, 2018). Langhans et al., (2016), for instance, showed that the probability of contamination of water supplies by debris flows are highly sensitive to the transmission ratio, which they defined as the proportion of clay-sized debris-flows material reaching the reservoir. Data and models that contribute towards better understanding of sediment transport through these channel networks are therefore important (Murphy, Czuba & Belmont, 2019). In settings where erosion events terminate on distinct fans, there is a history of data collection and empirical research (e.g. Michelini, Bettella & D'Agostino, 2017; Staley, Wasklewicz & Blaszczynski, 2006; Whipple & Dunne, 1992), and the sediment budget is largely constrained to the alluvial fan. However, in many cases, such as those described by Moody and Martin (2001) and Pelletier and Orem (2014), sediment from small headwaters is delivered into dendritic networks where they are available to be reworked immediately by flow processes within a larger catchment. The coupling between sediment supply from steep headwaters and routing and storage in fluvial channel networks has been explored theoretically (e.g. Benda & Dunne, 1997a; Benda & Dunne, 1997b), but field studies that examine sediment transport at these larger catchment scales are rare.

Concepts such as connectivity and sediment cascades have proved to be useful avenues for modelling sediment transport through such channel networks (Bracken, Turnbull, Wainwright & Bogaart, 2015; Cavalli, Trevisani, Comiti & Marchi, 2013; Czuba, 2018; Heckmann & Schwanghart, 2013; Lisenby, Croke & Fryirs, 2017; Parsons, Bracken, Poeppl, Wainwright & Keesstra, 2015; Wohl, 2017). However, the data on spatial patterns of deposition, erosion and transport in channel networks needed to develop these concepts for spatially explicit modelling of debris flows are lacking. The lack of such datasets is partly due to the low frequency of debris flow, but also because this domain falls between two disciplines of hillslope geomorphology and fluvial geomorphology. The spatial distributions of the dominant flow process and grain size of deposits are rarely quantified for debris-flow dominated, upland river systems. Quantifying these parameters and linking them to the dominant erosion process in the debris-flow domain is important for understanding how debris-flow processes shape the landscape (Tucker & Hancock, 2010), impact on downstream habitats (Harris, et al., 2015; Roghair, Dolloff & Underwood, 2002), and lead to water quality issues (Dahm, et al., 2015).

This study is motivated by the need for quantification and improved understanding of sediment transport and deposition in an upland channel network that receives sediment from episodic debris flows in small tributary catchments. Our data collection is focused on a post-fire debris flow, which occurred in the Washington Creek catchment, a tributary to the Ovens River in SE Australia. The objectives of the study are twofold:

- To quantify volume and composition of sediment deposited within a small headwater stream that links debris-flow producing headwaters to the Ovens River.
- To construct a sediment budget using new measurements of channel deposition and existing empirical relations for predicting erosion and deposition by post-fire debris flows.

Informed by the sediment budget, we estimate the net export of sediment out of the Washington Creek catchment to the Ovens River. Moreover, with data on grain size distribution in deposits, we determine the degree with which fine sediment is preferentially transported through the arterial drainage network.

2. Methods

2.1 Geomorphic setting and the 2013 post-fire debris flow

The 14 km^2 Washington Creek catchment is a tributary to the East Ovens River in northeast Victoria, southeast Australia (Figure 1). Washington Creek drains north from the base of Mt Hotham in the SE Australia alpine region, which form parts of the Great Dividing Range that separates the coastal rivers in the south from the greater Murray River basin to the north. The elevation ranges from 1800 m a.s.l. at the catchment divide to 600 m a.s.l. at the outlet. Mean annual precipitation is about 1600 mm with the upper catchment receiving snow during the winter months of June to August. Vegetation is dominated by eucalyptus forests, varying from dry mixed-species sclerophyll forest at low elevations to alpine woodlands (*Eucalyptus pauciflora*) and grasslands at higher elevations (> 1400 m). There is a band of alpine ash (*Eucalyptus delegatensis*), a wet sclerophyll forest, at intermediate elevations (1100 to 1400 m). Fire return intervals vary from several decades in the dry sclerophyll forest at lower elevations to 100 years or more in the higher elevation forests that receive higher rainfall (McCarthy, Malcolm Gill & Lindenmayer, 1999).

The underlying bedrock in the catchment consist of marine sedimentary silt and mudstones. Hillslopes in the headwaters are steep (30-45 degrees) and long (150-200 m). Soil thickness in this type geology and landform are typically in the order of 0.5 - 1 m (Inbar, Nyman, Rengers, Lane & Sheridan, 2018). A stream network was constructed from a 10 m digital elevation model (DEM). The stream order of this network was calculated based on Strahler stream order classification, and where 1st order stream channels begin at the base of small zero-order convergent hollows (drainage area ~ 2 ha). From this, we define the arterial drainage network as the 4th and 5th order stream channels. The slope of the arterial channels in Washington Creek decrease from 0.3 m m^{-1} at the start of the 4th stream order channel to 0.1 m m^{-1} at the junction with East Ovens River, where Washington Creek is a 5th stream order channel. The 1-3rd stream order channels in these geologic setting tend to fill with colluvium between debris-flow events, which typically scour the channel to bedrock when they occur. In the lower arterial channels, the channel bed is a mixture of bedrock, debris-flow fans and alluvial deposits.

In February 2013 a wildfire south of Harrietville burnt around 15,000 hectares of forest, covering most of the Upper Ovens catchment (Figure 1). At the higher elevations of the Washington Creek catchment, most of the forest was crown burned. Dry forest at the lower hillslopes was burned to crown scorch (leaves damaged but not burned). At lower elevations, the fire was mainly an understory burn. Runoff-generated debris flows occurred in several small headwaters (Figure 2a) several weeks after the fire. These were triggered by a rainfall event (88 mm in total recorded at Mt Hotham) on the 27th of February 2013. The rainfall intensity varied throughout the day with a peak I_{30} of 44 mm h^{-1} (annual exceedance probability of 0.2) at 10 am. This peak was followed by rainfall with average intensity of 10 mm h^{-1} that lasted until 3 pm. The debris flows led to widespread damage to roads, infrastructure and downstream water quality impacts (EPA, 2013; Newton & Rossato, 2013). There was another intense rainfall event at Mt Hotham on 22nd of March the same year (I_{30} of 35 mm h^{-1}), which may have caused additional debris flows and reworking of sediment in the Washington Creek catchment.

<<<<<<<<<<<<<<<<<<<<Figure 1 here>>>>>>>>>>>>>>>>>>>>

2.2 Debris-flow deposition in arterial channels

2.2.1 Volume and spatial arrangement of deposits

Field measurements of deposition within the arterial stream network were obtained during a 2-week field campaign in November 2013, about 6 months after the debris flow occurred. Sediment in the channel had experienced some reworking in the time period between the debris flow and the field campaign. However, there were no days with 30-minute intensities greater than the rainfall intensity on the 27th of February 2013, when the debris flow occurred (Supporting Information Figure S1a). Sediment reworking was typically confined to a narrow incision (1 - 3 m wide) into the debris fans that had been deposited in the channel by the post-fire debris-flow event (Supporting Information Figure S1 b-e). Channel deposits were on average 19.9 m wide (minimum = 11.1 m; maximum = 34.7m), so the reworking was minor relative to the volume of debris-flow deposition. Importantly, the incised parts of the deposits provided reference points for measuring depth of deposits and vertical profiles from which grain size distribution of deposits could be sampled.

We measured the volume of 27 distinct deposits (Figure 2a) in the arterial 4th - 5th stream order channels. Two or three cross-sections, oriented perpendicular to the arterial channel, were measured at each deposit (Figure 2b). At each deposit, the cross-sections were spaced to obtain a representative measure of volume considering the variation in deposit morphology along the reach. Coordinate points in a cross-section were measured at centimetre accuracy (± 4 cm) using a Trimble R6 GNNS differential GPS in combination with a CX series Sokkia total station. Points along the cross-sections were collected at the major slope breaks over the cross-section. There are 77 cross-sections in total.

The original channel bed was reconstructed by linear interpolation between reference points that were identified in the field as the channel bed or banks prior to the debris-flow event. Surfaces with intact vegetation, root mats, or soil surface with a clearly defined O-horizon were commonly used as indicators of the channel bed. For each cross section, we collected 2 reference points on each channel bank, and somewhere between 3 and 8 in-channel reference points for the channel bed. The cross-sectional area of deposition (m^2) was calculated as the integral between the linearly interpolated original bed and the measured surface of deposition. The mean cross-sectional area (m^2) for each major deposit was calculated by averaging the measured cross-sectional areas (Figure 2b). Deposited volumes were obtained by the multiplication of the mean cross-sectional area with the length of a deposit.

<<<<<<<<<<<<<<<<<<<Figure 2 here>>>>>>>>>>>>>>>>>>>

The position and volume of deposits were plotted in relation to slope, S (m m^{-1}) and area, A (m^2), obtained from a from a 10 m resolution DEM. The S - A data from the channelized domain of Washington Creek catchment was fitted with an equation describing the curvilinear trend that exists between debris flow and fluvial domains (Eq 5. in Stock & Dietrich, 2003);

$$S = \frac{s_0}{(1+a_1 A^{a_2})} \quad (1)$$

Where s_0 = 0.7 m m^{-1}, α_1 = 0.17*10^{-3}, and α_2 = 0.68 (R^2 = 0.99, RMSE = 0.063). The curvature of Equation (1) was used to discriminate between fluvial and debris-flow domains and identify in which domain the deposits occurred (Supporting Information Figure S2).

2.2.2 Grain size distribution and flow classification of deposits

Grain size distributions of deposits were measured on exposed vertical profiles. Grains of diameter (d) 5 mm to 256 mm were counted using the Wolman pebble count approach (Wolman, 1954) on digital photographs, taken with a 14.1 MP Canon PowerShot G1X Camera. Digital photographs were taken from an area of approximately 1.2 m^2 from three profiles. Length scales were placed along the vertical and horizontal axis of the photograph. Grids (250 x 250 pixels) overlying each image were then created using the image processing toolbox in Matlab. The average length (mm) of pixels was determined for each photograph from the number of pixels along 10 x 5 cm length segments sampled from horizontal and vertical axes. Particle a-, and b-axis were measured from at least 100 grid locations in each image. This sampling likely resulted in some grain size underestimation due to burial and overlapping grains, but the method is shown to produce results that are similar to traditional field methods (Graham, Rollet, Piégay & Rice, 2010). Sediment (d < 5 mm) from each vertical profile was collected in sample bags and composited into a single sample of ~ 0.25 kg per deposit. The sediment was collected by holding a 10-litre bucket below the sampling location and using shovel to release sediment from different depths in the profile. These sediment samples of d < 5 mm were processed in the laboratory using dry sieving (1 mm ≤ d < 5 mm) and laser diffraction (d < 1 mm).

Grain size data from the Wolman pebble count, dry sieving and laser diffraction were combined based on the proportion of total deposit volume represented by each method. The proportion of grains in the Woman pebble count relative to the full particle size distribution (G_w) was determined from the ratio:

$$G_w = \frac{P_w}{P} \quad (2)$$

Where P_w is the count of grid points where d ≥ 5 mm and P is the total number of grid points in the image. The proportion of grains in the dry sieving fraction (1 mm ≤ d < 5 mm), G_s, was determined from:

$$G_s = \frac{M_{1 \le d < 5}}{M_{d<5}}(1 - G_w) \quad (3)$$

Where $M_{1 \le d < 5}$ is the mass of sediment that was measured by dry sieving, and $M_{d<5}$ is the total mass of the sediment sample analysed in the laboratory. This calculation assumes the same density for all dry sieved grains (1 mm ≤ d < 5 mm). The proportion of grains analysed using laser diffraction makes up the remaining fraction:

$$G_{lps} = 1 - G_s - G_w \quad (4)$$

With these proportions (G_w, G_s and G_{lps}) the grain size distribution from each method were combined to a single volumetric distribution that is directly linked to the measurement of the deposit volume. From this we calculated the proportion of clay & silt (d < 0.063 mm), sand & gravel (0.063≤ d >2 mm), and pebbles & cobbles (2 ≤ d < 256 mm) in each deposit.

The median grain size (d_{50}) and sorting were also calculated from the distributions. Sorting was calculated in units of phi (ϕ) as $(\phi_{84} - \phi_{16})/2$ (Folk & Ward, 1957). Sorting and d_{50} were calculated from the distribution of grains by mass, in order to facilitate comparison with published data. The grain size distribution by mass was obtained from the volumetric distribution by adjusting for different bulk densities of grains with d ≥ 10 mm (2200 kg m^{-3}; bulk density of sandstone) and grains with d < 10 mm (1450 kg m^{-3}; bulk density of soil cores sampled from debris-flow deposits in similar geologic settings in Nyman (2013)). A grain size threshold of 10 mm was considered appropriate for this calculation because grains < 10 mm were found to comprise 95% of the mass in the bulk density cores (diameter = 75 mm) used to sample fine debris-flow material (Nyman, 2013). Using information from grain size distributions, deposit morphology and structure we classified deposits as debris flow (DF) or hyperconcentrated flow (HCF) using the classification criteria outlined in Cannon (2001: Table 2).

2.3 Construction of sediment budget

2.3.1 General approach

A sediment budget was constructed using combination of new data on sediment deposition collected in Washington Creek, and empirical models of erosion and deposition developed as part of earlier studies on sediment delivery from debris flows in SE Australia (Nyman, et al., 2015). We use the new data and model to produce maps of erosion (E) and deposition (D) (in units of m). Based on these maps, the volume of sediment, V (m^3) at any given drainage area, A, was obtained by accumulating net erosion ($E - D$) in all contributing upstream cells $(x, y)_i$ using a D-8 flow routing algorithm:

$$V = r^2 \left(\sum_i (E(x,y)_i - D(x,y)_i \right) \quad (5)$$

where i are all upstream cells in the catchment that contribute to V, and r =10 m (DEM resolution).

Spatial information on erosion and deposition is required as input to Equation (5). Deposition in the arterial channel was mapped using the data on deposit volumes from the field survey at Washington Creek together with measurements of deposit widths that we obtained from high resolution aerial photography. All other components to the sediment budget were modelled using relations that describe erosion and deposition as functions of a stream power index, which is the product of *S* and *A*. These relations were developed using data from erosion surveys from 10 post-fire debris flows in sedimentary geology in dissected uplands in eastern Victoria (Nyman, et al., 2015) (Supporting Information Figure S3), which is a geomorphic region that encompasses the Washington Creek catchment. We rely on these relations to model *i*) erosion and deposition in channels and on hillslope upstream of the arterial channels, and *ii*) erosion in arterial channels. The assumption is that the relations are transferable and valid for the Washington Creek debris flow. Uncertainties associated with our estimates are propagated and reported in the budget. The Supporting Information provides detail on model testing, and the justification for our approach, using results from Nyman, *et al.* (2015) to model erosion and deposition at Washington Creek. Here we list the equations.

The local hillslope erosion depth, E_h (m), within the hillslope domain ($A \leq 1.3 * 10^4$ m^2) is:

$$E_h = 4.5 * 10^{-4} (SA)^{0.36} \quad (6)$$

E_h is set to 0 outside the hillslope domain. Deposition on hillslopes (D_h) is 30% of the erosion, calculated based on the concentration of Caesium-137 and Lead-210 in debris-flow deposits (Nyman, et al., 2015; Smith, et al., 2012):

$$D_h = 0.3E_h \quad (7)$$

Local channel erosion depth, E_c (m), within the channel domain ($1.3 * 10^4$ m^2 $< A \leq 1.4 * 10^7$m^2) of our study area is:

$$E_c = 4.1 * 10^{-4}(SA)^{0.52} \quad (8)$$

E_c is set to 0 outside the channel domain.

In-channel and levee deposition D_c (m), within the channel domain ($1.3 * 10^4$ m^2 $< A \leq 1.4 * 10^7$m^2) is:

$$D_c = 3.7 * 10^{-7}\ (SA)^{1.06} \quad (9)$$

The switch from hillslope to channel domains was based on the inflection point on the slope area curve, which indicates the location where hillslopes transition to channels (e.g. Montgomery & Foufoula-Georgiou, 1993; Staley, Wasklewicz & Kean, 2014).

Data on grain size distributions were used to evaluate the degree with which fine sediment were preferentially transported out of the catchment. This was achieved by comparing the grain size distribution of deposited material in the arterial channel with grain size distribution of sediment of the sediment that is eroded from hillslopes and colluvium in 1-3rd order stream channels. Grain size distribution of the eroded sediment (Table 1) is available from data collected in the Germantown Catchment (Nyman, et al., 2015), located ~15 km further south, and which has the same geology and soil type as the Washington Creek catchment. Methods used to characterise grain size distribution of source material, described in Nyman, *et al.*, (2015), comprise extensive sampling of channel and hillslope sources and analysis by sieving and pipette methods.

2.3.2 Volume of deposition and erosion in the arterial channel

Erosion in the arterial channel was modelled using Equation (8). The drainage areas contributing to the arterial channel is larger than the drainage areas of the catchments used in development of Equation (8). Erosion rates obtained using this method were therefore

validated by measurements of channel erosion and bank failure at 14 different locations within the arterial channels (Supporting Information Figure S3). Deposition in the arterial channel was determined with different methods depending on the type of deposition, which we determined during the field campaign. Based on our field observations, deposition in the reaches along the arterial channel were classified as; *i*) reaches with no deposition, *ii*) reaches with major deposits that were measured with cross-sections, and *iii*) reaches with minor deposits that were not measured with cross-sections (Supporting Information Figure S4a). In reaches with no deposition, D is 0. In reaches with major deposits, D equals the volume estimates obtained directly from the 77 cross-section measurements. In reaches with minor deposition, there are no direct cross-section measurements. For these we use a linear relation between deposit width (D_w) and deposit cross section area (D_A) to estimate D. The width of deposits was measured every 25 m along the arterial channel using aerial photography (15 cm resolution) collected on the 30th of April 2013, about one month after the debris flows. The relationship between D_A of deposits and D_w was obtained using data from locations where cross-section measurements were available (Supporting Information Figure S4b). Error introduced by this method is accounted for in the sediment budget using the root mean square error of the regression between D_A and D_w.

2.3.3 Volume of deposition and erosion in source areas

Sediment delivery into the arterial channels was estimated for debris-flow producing tributary catchments. We refer to these tributary catchments as debris-flow source areas. Debris-flow source areas were mapped from orthorectified aerial imagery with 15 cm resolution based on channels that were visibly scoured to bedrock and that connected to with arterial channels (Figure 2a). In the smallest source areas, debris-flow producing headwaters connect with arterial channel via a single 1st stream order channel. In larger sources areas, the debris-flow producing headwaters connects with the arterial channel via a network of 1 - 3rd stream order channels. The identification of debris-flows from aerial imagery was validated with evidence collected during the field campaign, where we inspected each tributary and noted the presence or absence of levees, channel scour and scarred tree trunks. Thirty-two distinct debris-flow source areas (0.01 km^2 < A < 0.78 km^2) were identified and covered a total surface area of 5.2 km^2, which correspond to 37% of the total catchment area (Figure 2a).

In our approach to estimating sediment input from source areas, we assume that presence or absence of a debris flow is the key point to consider in determining sediment input from

tributaries. In SE Australian forests, debris flows produce sediment loads that are two orders of magnitude higher than sediment delivery from other post-fire erosion processes (Sheridan, et al., 2016). For example, the largest post-fire erosion event after higher severity fire in the East Kiewa catchment (20 km to the north east of Washington Creek, on similar geology), where no debris flow occurred, was 1.3 Mg ha^{-1} (Lane, Sheridan & Noske, 2006). That event occurred in response to a rainfall intensity (I_{30} = 53 mm h^{-1}), similar to that which caused debris flows in the Washington Creek catchment. By comparison, the sediment load from debris flows in this landform is on average 170 Mg ha^{-1} (Nyman, et al., 2015). Taking these best available data on sediment load as approximations, and the proportion of Washington Creek catchment comprising debris-flow tributaries (37%), the contribution from tributaries without debris flow is 1.5% of what is produced by debris flows. We use these existing data and approximations to justify the assumption that sediment input from tributaries without debris flows is negligible. By mapping debris-flow producing tributaries we implicitly consider effects of fire severity, aridity, topography and the spatial distribution of rainfall intensities because these factors are strongly linked to debris flow occurrence (Nyman, et al., 2015).

2.3.4 Calculating uncertainty in the sediment budget

The total uncertainty ($U\_V_{catchment}$) in the estimated sediment efflux was obtained by propagating the uncertainties in each component of the sediment budget:

$$U\_V_{catchment} = \sqrt{U\_V_h{}^2 + U\_E_{c\_tot}{}^2 + U\_D_{c\_tot}{}^2 + U\_E_{c_a}{}^2 + U\_D_a{}^2} \quad (10)$$

Where U_V_h is the uncertainty in total hillslope sediment delivery, $U\_E_{c\_tot}$ is uncertainty in modelled channel erosion in sources areas, $U\_D_{c\_tot}$ is uncertainty in modelled deposition in sources areas, $U\_E_{c_a}$ is uncertainty in modelled channel erosion in arterial channel, and U_D_a is the uncertainty in estimates of deposition in arterial channel (details on the calculation of each error term are described in Supporting Information).

The main sources of uncertainty considered in the terms above resulting from *i*) uncertainties in Equations 6 - 9 used to model erosion and deposition, *ii*) assumptions regarding the shape of pre-existing channel, which was used to obtain channel cross-section areas, and *iii*) extrapolation of deposition to channel reaches that were not measured. In some cases, the uncertainty term was quantified using the root mean square error (RMSE) from regressions

that were used in constructing the budget. In other cases, when the error stems from assumptions in the measurement technique, the uncertainty was quantified based on the sensitivity of the measurement to assumptions. For example, in calculating deposition from cross-sections we assume channel shape can be reconstructed from points along the cross sections that represent the pre-exiting channel bed. Uncertainty associated with this assumption was quantified by calculating the standard deviation of cross-section area obtained assuming different channel profiles (Supporting Information Figure S5).

3. Results

3.1 Deposit volume and sediment composition in the arterial channels

The volume of measured deposits ranged from 27 m^3 to 1573 m^3 (average = 473 m^3) (Figure 3a; Table 2). Several of the large deposits were clustered around distinct breaks in the slope-area curve (Figure 3a), which correspond with the location of stream junctions. Large deposits occurred at a wide range of slopes (0.02 – 0.31 m m^{-1}), but most deposition (56%) occurred in a relatively narrow range of channel slopes (0.08 - 0.15 m m^{-1}). Twenty out of the 27 deposits were classified as debris flows (DF) (red open circles Figure 3a), while seven deposits were classified as hyperconcentrated flow (HCF) (blue open circles Figure 3a). Based on the curvature of Equation (1), the transition from debris flow to fluvial domains occurs at a drainage area of ~ 80 x 10^6 m^2 and channel slope of 0.07 m m^{-1} (Supporting Information Figure S2). In the fluvial domain 55% of deposits were classified as HCF while in the debris-flow domain HCF only make up 13% of deposits. Thus, most of the debris-flow type deposits were deposited in the debris-flow domain, and most of the hyperconcentrated flow deposits were present in the fluvial domain.

The median grain size in debris flow and fluvial deposits are similar (8.5 mm and 7.3 mm, respectively. Correlation of d_{50} show some trends in grain size with drainage area, but these relations are different in the fluvial and debris-flow domains. In the debris-flow domain, d_{50} increases with A (Pearson r =0.55, $p < 0.05$) (Figure 3b). In the fluvial domain, however, there is no significant correlation. Sorting (σ_ϕ) shows no correlation with A (Figure 3b) and no difference between deposits classified as DF (σ_ϕ = 1.67) and HCF (σ_ϕ = 1.7). The coefficient of fixation (d_{50}/S) (Figure 3c) appears to increase and then decrease with A. There is a positive correlation in the DF domain (Pearson r = 0.51, $p < 0.05$) and negative correlation in the fluvial domain (Pearson r= -0.48, $p < 0.1$) (Figure 3c). The peak in d_{50}/S at A~10 km^2 is

where flow domains go from debris flow to fluvial processes (as determined from the curvature in Equation (1).

As a proportion of volume, the deposits contained on average 1% silt and clay (d < 0.063 mm), 12% sand (0.063 mm < d < 2 mm) and 86% gravel, pebbles and cobbles (2 mm < d < 256 mm). These proportions varied along the drainage area (Figure 3d). Deposits with highest fine sediment (~3%) fraction were located just upstream of the major junctions, which were also associated with break in slopes (Figure 3a). Silts and clays are largely absent from of the deposits located in the middle and lower arterial channels ($A > 4.3*10^6$ m^2). The proportion of sand, silt and clays (d < 2 mm) in deposits is ~10 times lower compared to the proportion in hillslope and channel source areas (Figure 4).

<<<<<<<<<<<<<<<<<<<Figure 3here>>>>>>>>>>>>>>>>>>>>>

<<<<<<<<<<<<<<<<<<<Table 2 here>>>>>>>>>>>>>>>>>>>>>

<<<<<<<<<<<<<<<<<<<Figure 4 here>>>>>>>>>>>>>>>>>>>>>

3.2 Sediment budget

Estimated erosion and deposition in Washington Creek are reported as volumes per grid cell in the 10 m DEM (Figure 5). The average volume of erosion in the arterial channel, modelled using Equation (8), was 41 m^3 (ranging from 0 – 131 m^3) (Figure 5a). Reaches of the arterial channel where there is no erosion stems from the assumption that channel is not eroding in the location where we observed large deposits. The total volume of erosion in the arterial channel is 31 x 10^3 m^3. The volume of deposition in the arterial channel was lognormally distributed with a mean of 38 m^3 and standard deviation of 7.9 m^3 (range: 0 - 311 m^3) (Figure 5b). The total deposition in the arterial channel was 39 x 10^3 m^3, of which 44% was in the major deposits that were measured with cross sections, and which are shown in Figure 3a. The remaining deposits are distributed in depositional environments between these major deposits. Net erosion in the arterial channel, calculated as the difference between erosion and deposition in 10m grid cells of the DEM, varies from -240 m^3 (deposition) to 131 m^3 (erosion) (Figure 5c). In the mid- and north tributaries (shown in Figure 2a), there is net deposition through much of the arterial channel, with a net sediment gain between 10 and 100 m^3 per cell. In the southern tributary there is mostly net erosion, with net deposition in some

localised reaches. Over the total arterial channel length, the rate of deposition and erosion were 26 m^3 m^{-1} and 20 m^3 m^{-1}, respectively. Average width of deposits in the arterial channel is 19.9 m (ranging from 11-35m).

Debris-flow source areas upstream of the arterial channels are located primarily on north or north-west facing slopes that were vegetated with dry open or alpine forest, and which were burned at high fire severity. Debris flows are mostly absent in the northern section of the Washington Creek catchment, where *i*) the forest is wetter due to southerly aspects, and *ii*) where the fire severity was lower (Figure 1). Patterns of local erosion and deposition in source areas are dictated entirely by the stream power index, calculated from Equations 6 – 9. They both increase with increasing drainage area and are higher in the channelized domain compared to hillslopes. The volume of sediment originating in the 32 debris-flow source areas, modelled from Equation (5), varies between 75 m^3 and 7200 m^3. In terms of sediment yield, the modelled sediment volumes correspond to 123 - 311 Mg ha^{-1}. Total sediment originating from hillslope source areas obtained with Equation 6 - 7 was 43 x 10^3 m^3. Debris-flow material originating from 1st-3rd stream-order channels in debris-flow source areas was 35 x 10^3 m^3. The model predicts an overall 55% and 45% split between hillslope and channel sediment sources.

<<<<<<<<<<<<<<<<<<<Figure 5 here>>>>>>>>>>>>>>>>>>>>>

Our estimates of net erosion are used to accumulate sediment volumes (Figure 5c). These are in turn summarised into sum of volumes along the flow direction (Figure 5d), and a sediment budget (Figure 6). The total volumes of erosion and deposition throughout the catchment were 109 ± 36 x 10^3 m^3 and 48 ± 23 x 10^3 m^3, respectively, giving a sediment export from the catchment of 61 ± 40 x 10^3 m^3 (Figure 6). There are similar contributions of hillslopes (43±14 x 10 m^3), 1-3rd stream order channels (35±12 x 10 m^3) and the arterial 4-5th stream order channels (31±17 x 10 m^3) to the total volume of erosion. Deposition (39±17 x 10 m^3) within the arterial channel was slightly higher than erosion (31±17 x 10 m^3), which means there is a net sediment gain of about 8 x 10^3 m^3 in the arterial channel. The relation between debris-flow volume and catchment area is non-linear, as indicated by the exponent (0.73) in a power-law of volume vs drainage area ($V = 0.35A^{0.73}$; R^2=0.97). The volumetric efflux

equates to a sediment yield of 78 t ha^{-1}, assuming channel bulk density to be similar to measurements of channel sediments (~1800 kg m^{-3}) in the nearby catchment at Germantown (Nyman, 2013).

<<<<<<<<<<<<<<<<<<<Figure 6 here>>>>>>>>>>>>>>>>>>>>>

Fine-grained sediment (clays and silts; d < 0.063 mm), and to a lesser degree sand, were preferentially transported out of the catchment compared to other sized material. In the measured deposits , the clay and silt fraction (range = 0.07-3.2 %; mean = 0.9 %) was on average 20 times lower than clay and silt fraction content in the hillslope and channel source areas (~20%), which we determined using measurement of sediment from same geology at the nearby Germatown catchment (Nyman, 2013). Using these measurements as a reference, the overall ratio of exported to eroded material in the clay and silt fraction was 0.89. For all grain sizes the ratio is 0.56.

4. Discussion

4.1. Sediment deposition and transport in the arterial channel

Debris flows were present throughout the arterial channels of the study catchment, and were sustained in the lower reaches, even where the channel slope was relatively low (0.02 - 0.07 m m^{-1}). The slopes in these lower reaches are comparable to typical slopes (0.05 - 0.2 m m^{-1}) for debris-flow deposition (Benda & Cundy, 1990; Guthrie, et al., 2010). Deposition of debris-flow material occurred mainly in localized pockets of reduced stream power, such as on the inside of channel bends, behind log and boulder jams and at junctions with locally reduced channel gradient. Despite these localized, sometimes substantial deposits, the flow was dominated by debris flow throughout most of the channel network (Figure 3a). Deposits that were indicative of hyperconcentrated flows were increasingly common in the lowest reaches of the arterial channel, near the confluence with the Ovens River. This shift in dominant flow type corresponds with the transition from debris flow to fluvial domains, as determined from curvature of the slope-area curve (Stock & Dietrich, 2003). Mechanisms for this shift is probably linked to dilution of the flow by the accumulation of surface runoff from

non-debris-flow producing tributaries, reduced bed grade and widening of the arterial channel. These all reduce the capacity to sustain the coarse-grained flow front typical of debris flow (Jakob & Hungr, 2005; Pierson, 2005).

Despite the shift from debris flows to hyperconcentrated flow as the dominant flow process, there were only minor catchment-wide change in grain size distribution in deposits (Figure 3b, Table 2). The absence of sorting along the longitudinal stream profile indicates that the flow competence remained sufficiently high to transport coarse grains, as granular fronts in the case of debris flows or as bedload in hyperconcentrated flows (Iverson, 1997; Lowe, 1979). The coefficient of fixation (d_{50}/S) increases up to the beginning of the fluvial domain, from whereon it decreases again (Figure 3c). This indicates that the ratio of resisting forces (weight) to propelling forces (slope) of the sediment bed increases, then decreases with area. Within the DF domain, the amount of work done by flow to shift sediment increases with area, because volumes of both water and sediment are increasing. Beyond the DF domain, the amount of work done by the flow to shift sediment decrease with area. Larger area equals less force in the flow, because the sediment is depositing, creating lower density flow. Thus, as the flow shifts from DF to HCF, there is a decrease in the force available to transport sediment. The drainage area where this shift occurs is also where our model predicts equal rates of deposition and erosion (Supporting Information Figure S3). Together, the model and our interpretation of the deposits, indicate that contemporary sediment transport processes are commensurate with the flow domains determined from topographic signature that has evolved over geologic time scales.

Prior investigations of deposition in arterial channels after wildfire indicate that the longitudinal slope profile may account for the large differences in connectivity between the debris-flow and fluvial domains. For example, Pelletier and Orem (2014) mapped erosion and deposition during a debris-laden flow over a large area (up to 20 km^2) at high resolution using airborne LiDAR. They found that the sediment volume increase was directly proportional to contributing area, indicating efficient transport of sediment through the catchment and limited storage in the drainage network, which was relatively steep ($S > 0.1$). A contrasting example is the Spring Creek Catchment (26.8 km^2) in Colorado where work by Moody and Martin (2001) and Moody (2017) showed that the arterial channel could accommodate large volumes of sediment, thereby creating dis-connectivity, and limiting catchment-scale sediment export. Of the total 1.1 million m^3 sediment input, 0.74 million m^3 (or 70%) remained in storage as a

superslug (Moody & Martin, 2001). The slope of the arterial channel at Spring Creek outlet (0.02-0.05 mm^{-1}) was half of that in the catchment surveyed by Pelletier and Orem (2014).

Our study falls in between these two studies. Storage within the channel was ~44% of the total erosion, lower than in Spring Creek (Moody & Martin, 2001). Based on our reconstruction of erosion and deposition in the Washington Creek Catchment, the exponent of the power-law relation between debris-flow volume and drainage area was 0.73, so transport was less efficient than in the Pelletier and Orem (2014). This exponent indicates that, in contrast with Pelletier and Orem (2014), there are scale-effects within the catchment whereby sediment yield (volumes per unit area) decreases with area. Our results are more consistent with those of Cannon, *et al* (2010) and Gartner, *et al.*, (2014), where debris-flow volumes scale as a power-law relation with drainage area to an exponent between 0.49 and 0.6. Over the long-term, this scaling in V with drainage area is expected as it maintains the steady state fluvial scaling where slope and drainage area are balanced (Tucker & Bras, 1998). For individual erosion events, however, the strength of scaling depends on spatial arrangement of erosion and deposition. At Washington Creek, scaling could stem from both topographic and hydrologic controls, which are structural and functional component of connectivity (Bracken, et al., 2015). A key feature with respect to topographic controls, evident in Figure 3a, are the large deposits located around breaks in slope at stream junctions. These depositional environments accommodate large volumes of sediment, creating dis-connectivity in sediment transport between debris-flow source areas and the catchment outlet. The hydrologic controls on scaling are linked to spatial arrangement of debris-flow producing tributaries. In SE Australia, this arrangement of debris-flow producing tributaries is often linked to aridity, with dry north (equatorial) facing slopes being more likely to produce surface runoff and debris flows than wetter south-facing slopes (Noske, Nyman, Lane & Sheridan, 2016; Van der Sant, et al., 2018). Fire severity is another source of variation, with high severity burns more likely to produce a debris-flow response (Cannon, et al., 2010; Gartner, et al., 2008; Nyman, et al., 2015; Staley, et al., 2017). The spatial patterns of debris-flow producing tributaries is important for the catchment-scale response and a major consideration when making prediction about debris-flow dynamics and sediment transport for any given event. For instance, a different distribution of rainfall intensity or fire severity could have led to a very different arrangement of debris-flow source areas, which in turn could exacerbate or moderate the debris-flow response through the arterial channel.

4.2 Preferential transport of fine material

The low silt and clay content in the channel deposits (1%) compared to source areas (20%) illustrates the importance of grain size in sediment connectivity. Fine sediments are preferentially transported out of Washington Creek. Similar results have been noted previously in relation to the preferential transport of clay-sized material (Benda & Dunne, 1997b; Pierson, 2005). This has been linked to the distribution of sediment within debris-flow surges with fine-grained and water-rich tails (Hungr, 2000; McCoy, et al., 2010), that are likely to continue moving after the onset of coarse-grained deposition. At Washington Creek, the rainfall continued at relatively high intensity (10 mm hr^{-1}) for 4.5 hrs, contributing to runoff for several hours after the initial debris-flow surge. This immediate exposure of deposits to reworking by runoff would have contributed to transport of fines. There was clear evidence in the field that the fines were washed out of deposits (Figure 7). Reworking by stream flow in the period between the debris flow event and the field campaign (including runoff from the intense rainfall event on March 22nd) would have contributed to the fine sediment transport from areas of the deposits where the new channel is forming. The implications of fine sediment transport for downstream water quality can be large. In a sensitivity analysis by Langhans et al. (2016), for instance, the prediction of clay inputs to a water supply reservoir were very sensitive to the transmission ratio, which is the efficiency with which fine sediment is transported out of a catchment were a debris flow occurred. Once fines reach a river, they can be transported a very long distance downstream as demonstrated by Lyon and O'Connor (2008) after a debris flow in another tributary to the Ovens River.

<<<<<<<<<<<<<<<<<<<Figure 7 here>>>>>>>>>>>>>>>>>>>>>

4.3 Geomorphic impact of debris flows

The geomorphic significance of the debris flow depends on the reference time-scale. The debris flow ($61 \pm 40 \times 10^3$ m^3; 78 Mg ha^{-1}) corresponds to 400-800 years of background erosion, which is low in SE Australian forests, typically ranging from 0.1 to 0.2 Mg ha^{-1} yr^{-1} (Lane, et al., 2006; Smith, Sheridan, Lane & Bren, 2011). Catchment-scale denudation caused by the debris flow is 3.4 mm assuming bulk density of 1800 and 2200 kg m^{-3} for channel sediment and bedrock, respectively. With denudation rates over the last 30 000 years ranging between 15 and 25 mm kyr^{-1} for southeast Australia (Heimsath, Chappell, Dietrich, Nishiizumi & Finkel, 2001), this event equates to approximately 150-220 years of denudation. The discrepancy between short-term and long-term significance arise from these

extreme events, which are rare, but which dominate long-term sediment yields (Kirchner, et al., 2001; Tomkins, et al., 2007).

In a simplistic case, the combined probability of fire and the rainstorm (assuming they are independent) can be used to estimate return interval of such an event. Taking a fire return interval of 50 years, which is typical for high-severity fire in these type of forests (Kennedy & Jamieson, 2007; McCarthy, et al., 1999), and a rainfall exceedance probability of 0.2 (equal to this recent event) gives a debris-flow return interval of about 250 years, within the range reported in earlier studies from the region (Jones, Nyman & Sheridan, 2014; Smith, et al., 2012; Worthy & Wasson, 2004). At this frequency the average denudation due to fire-related erosion events (13.6 mm kyr^{-1}) would add to contemporary background rates (4.5 - 9.0 mm kyr^{-1}, Lane 2006) and thus bring the erosion regime into agreement with measured denudation rates (15 and 25 mm kyr^{-1}). This simple analysis assumes that the current fire and rainfall regime represent the conditions that cause debris-flows over geological timescales. It also assumes that the sediment yields from debris flows are largely controlled by sediment availability and not variation in rainfall intensities. Notwithstanding these assumptions, the analysis illustrates how extreme events can resolve discrepancies between short and long-term denudation and reinforces the importance of episodic erosion for sediment transport.

Newly deposited sediments by debris flows will likely reside in the channel network for many years where it undergoes remobilisation, redistribution and weathering (Lancaster & Casebeer, 2007; Lancaster, Underwood & Frueh, 2010; Moody, 2017; Reneau, Katzman, Kuyumjian, Lavine & Malmon, 2007). Generally, sediment residence times in the arterial channels are higher than the residence times of sediment in the upstream debris-flow affected headwater channels (Lancaster & Casebeer, 2007). However, the newly deposited sands may act as a long-term source of sediment to downstream reaches for many years after the event (Moody, 2017). In the short- to medium term the distribution of sediment within the channel network is likely to be in state of disequilibrium with the flow regime and therefore subject to a period of reworking. The amount of reworking depends on the post-event flow, as well as the rate of vegetation recovery along the stream (Moody, 2017; Reneau, et al., 2007). Reworking is likely to cause increased sediment yields during high flows. However, with clay and silt having been transported away from the deposits, much of the potential increases in sediment yield will be bedload transport (Reneau, et al., 2007). The sediment budget indicates sediment storage in the channel has increased by 8×10^3 m^3. With this estimate and

an assumed debris-flow return interval of 250 years, the channel erosion would need to be in the order of 0.05 Mg ha^{-1} yr^{-1} to be in balance with episodic input from headwater tributaries.

Conclusions

This study set out to examine how sediment is transported from small headwaters (< 1 km^2) through the arterial channel of a larger catchment (14 km^2) by a post-fire debris-flow. The results show strong agreement between transport processes inferred from grain size distributions and the flow domains inferred from slope area curves. Hyperconcentrated flow emerge as the more dominant process towards the catchment outlet where the curvature of the slope-area curve also indicates the catchment transitions from debris-flow to fluvial domains. This shift corresponds to a change in efficiency of the flow as indicated by the ratio of median grain size to channel slope. However, there was no systematic longitudinal sorting or changes in grain size of in-stream deposits. Our estimates of deposition and erosion in the channel network (39±17 x 10^3 m^3 and 31±17 x 10^3 m^3, respectively) suggest sediment storage in the arterial channel increased by 8 x 10^3 m^3. This is likely to promote higher sediment yields in the short- to medium term, while the channel sediments are subject to reworking. A large proportion (~89%) of eroded fines (< 63 µm) appear to have been exported from the catchment, however, which means that the elevated sediment yields will be largely bedload transport of sands and gravel.

Acknowledgements

Funding received from the Australian Research Council (LP150100654), the Melbourne Water Corporation and the Department of Environment, Land, Water and Planning (DELWP). Reviewers on earlier versions of the manuscript provided very valuable suggestion for improvements. Philip Noske, Glenn Dunshea and Nuosha Zhang helped with field work. Data from this study can be made available on request. The authors have no conflict of interest to declare.

References

Benda, L., & Dunne, T. (1997a). Stochastic forcing of sediment supply to channel networks from landsliding and debris flow. *Water Resources Research, 6*, 2849-2863. doi:10.1029/97WR02388

Benda, L., & Dunne, T. (1997b). Stochastic forcing of sediment routing and storage in channel networks. *Water Resources Research, 33*, 2865-2880. doi:10.1029/97WR02387

Benda L.E., & Cundy, T.W.. (1990). Predicting deposition of debris flows in mountain channels. *Canadian Geotechnical Journal, 27*, 409-417. doi:10.1139/t90-057

Bladon, K. D., Emelko, M. B., Silins, U., & Stone, M. (2014). Wildfire and the future of water supply. *Environmental Science & Technology, 48*, 8936-8943. doi:10.1021/es500130g

Bracken, L., Turnbull, L., Wainwright, J., & Bogaart P. (2015). Sediment connectivity: a framework for understanding sediment transfer at multiple scales. *Earth Surface Processes and Landforms, 40*, 177-188. doi:10.1002/esp.3635

Cannon, S.H. (2001). Debris-flow generation from recently burned watersheds. *Environmental & Engineering Geoscience, **7***, 321-341. doi:10.2113/gseegeosci.7.4.321

Cannon, S. H., Gartner, J. E., Rupert, M. G., Michael, J. A., Rea, A. H., & Parrett, C. (2010). Predicting the probability and volume of postwildfire debris flows in the intermountain western United States. *Geological Society of America Bulletin*, *122*, 127-144. doi:10.1130/b26459.1

Cavalli, M., Trevisani, S., Comiti, F., & Marchi, L. (2013). Geomorphometric assessment of spatial sediment connectivity in small Alpine catchments. *Geomorphology, **188**,* 31-41. doi:1016/j.geomorph.2012.05.007

Czuba, J.A. (2018). A Lagrangian framework for exploring complexities of mixed-size sediment transport in gravel-bedded river networks. *Geomorphology*, 321, 146-152. doi: 10.1016/j.geomorph.2018.08.031

Dahm, C. N., Candelaria-Ley, R. I., Reale, C. S., Reale, J. K., & Van Horn, D. J. (2015). Extreme water quality degradation following a catastrophic forest fire. *Freshwater Biology, 60*, 2584-2599. doi:10.1111/fwb.12548

DeLong, S. B., Youberg, A. M., DeLong. W. M., & Murphy, B. P. (2018). Post-wildfire landscape change and erosional processes from repeat terrestrial lidar in a steep headwater catchment, Chiricahua Mountains, Arizona, USA. *Geomorphology, 300*, 13-30. doi:1016/j.geomorph.2017.09.028

EPA. (2013, 28 Feb). Emergency services respond to Harrietville landslide. Victoria EPA. Retrieved from https://www.epa.vic.gov.au/

Folk, R. L., & Ward, W. C. (1957). Brazos River bar [Texas]; a study in the significance of grain size parameters. *Journal of Sedimentary Research, 27*, 3-26. doi: 10.1306/74D70646-2B21-11D7-8648000102C1865D

Gartner, J. E, Cannon, S. H., & Santi P. M. (2014). Empirical models for predicting volumes of sediment deposited by debris flows and sediment-laden floods in the transverse ranges of southern California. *Engineering Geology, 176,* 45-56. doi: 10.1016/j.enggeo.2014.04.008

Gartner, J. E., Cannon, S. H., Santi, P. M., & Dewolfe, V. G. (2008). Empirical models to predict the volumes of debris flows generated by recently burned basins in the western U.S. *Geomorphology, 96,* 339-354. doi:10.1016/j.geomorph.2007.02.033

Gomi, T., Sidle, R. C., & Richardson, J. S. (2002). Understanding processes and downstream linkages of headwater systems. Bioscience **52**: 905-916. doi:10.1641/0006-3568(2002)052[0905:UPADLO]2.0.CO;2

Graham, D. J., Rollet, A-J., Piégay, H., & Rice, S. P. (2010). Maximizing the accuracy of image-based surface sediment sampling techniques. *Water Resources Research, 46,* doi:10.1029/2008WR006940

Guthrie, R., Hockin, A., Colquhoun, L., Nagy, T., Evans, S., & Ayles C. (2010). An examination of controls on debris flow mobility: Evidence from coastal British Columbia. *Geomorphology, 114,* 601-613. doi:10.1016/j.geomorph.2009.09.021

Harris, H. E., Baxter, C. V., & Davis, J. M. (2015). Debris flows amplify effects of wildfire on magnitude and composition of tributary subsidies to mainstem habitats. *Freshwater Science, 34,* 1457-1467. doi:10.1086/684015

Heckmann, T., & Schwanghart, W. (2013). Geomorphic coupling and sediment connectivity in an alpine catchment — Exploring sediment cascades using graph theory. *Geomorphology, 182,* 89-103. doi:10.1016/j.geomorph.2012.10.033

Heimsath, A. M., Chappell, J., Dietrich. W. E., Nishiizumi, K., & Finkel, R. C. (2001). Late Quaternary erosion in southeastern Australia: a field example using cosmogenic nuclides. *Quaternary International 83-85,* 169-185. doi:10.1016/s1040-6182(01)00038-6

Hungr, O. (2000). Analysis of debris flow surges using the theory of uniformly progressive flow. Earth Surface Processes and Landforms **25**: 483-495. doi:10.1002/(sici)1096-9837(200005)25:5<483::aid-esp76>3.0.co;2-z

Inbar. A., Nyman, P., Rengers, F. K., Lane, P. N. J., & Sheridan, G. J. (2018). Climate Dictates Magnitude of Asymmetry in Soil Depth and Hillslope Gradient. *Geophysical Research Letters, 45,* 6514-6522. doi:10.1029/2018GL077629

Iverson RM. (1997). The physics of debris flows. *Reviews of Geophysics 35,* 245-296. doi: 10.1029/97RG00426

Jakob, M., & Hungr, O. (2005). Debris-flow hazards and related phenomena. Springer. doi:10.1007/b138657

Jones, O., Nyman, P., & Sheridan, G. (2014). Modelling the effects of fire and rainfall regimes on extreme erosion events in forested landscapes. *Stochastic Environmental Research and Risk Assessment, 8,* 1-11. doi:10.1007/s00477-014-0891-6

Kean, J. W., McCoy, S. W., Tucker, G. E., Staley, D. M., & Coe, J.A. (2013). Runoff-generated debris flows: Observations and modeling of surge initiation, magnitude, and frequency. *Journal of Geophysical Research: Earth Surface, 118,* 2190-2207. doi:10.1002/jgrf.20148

Kennedy, A., & Jamieson, D. (2007). Ecological Fire Management in North East Victoria. In *The Joint AFAC/Bushfire CRC Conference*: Hobart, Tasmania.

Kirchner, J. W., Finkel, R. C., Riebe, C. S., Granger, D. E., Clayton, J. L., King, J. G., & Megahan, W.F. (2001). Mountain erosion over 10 yr, 10 k.y., and 10 m.y. time scales. *Geology, 29,* 591-594. doi: 10.1130/0091-7613(2001)029<0591:MEOYKY>2.0.CO;2

Lancaster, S. T. (2008). Evolution of sediment accommodation space in steady state bedrock-incising valleys subject to episodic aggradation. *Journal of Geophysical Research: Earth Surface, 113,* F04002. doi:10.1029/2007JF000938

Lancaster, S. T., & Casebeer, N. E. (2007). Sediment storage and evacuation in headwater valleys at the transition between debris-flow and fluvial processes. *Geology, 35,* 1027-1030. doi:10.1130/G239365A.1

Lancaster, S. T., Underwood, E. F., & Frueh, W.T. (2010). Sediment reservoirs at mountain stream confluences: Dynamics and effects of tributaries dominated by debris-flow and fluvial processes. *Geological Society of America Bulletin, 122,* 1775-1786. doi:10.1130/B30175.1

Lane, P. N. J., Sheridan, G. J., & Noske, P. J. (2006). Changes in sediment loads and discharge from small mountain catchments following wildfire in south eastern Australia. *Journal of Hydrology, 331,* 495-510. doi:10.1016/j.jhydrol.2006.05.035

Langhans, C., Smith, H. G., Chong, D. M. O, Nyman, P., Lane. P. N .J., & Sheridan, G. J. (2016). A model for assessing water quality risk in catchments prone to wildfire. *Journal of Hydrology, 534,* 407-426. doi:1016/j.jhydrol.2015.12.048

Lisenby, P. E., Croke, J., & Fryirs, K. A. (2017). Geomorphic effectiveness: a linear concept in a non-linear world. *Earth Surface Processes and Landforms, 43,* 4-20. doi:10.1002/esp.4096

Lowe DR. 1979. Sediment gravity flows: their classification and some problems of application to natural flows and deposits. *Special Publications of SEPM, 27,* 75-82.

Lyon, J. P., & O'Connor, J. P. (2008). Smoke on the water: Can riverine fish populations recover following a catastrophic fire-related sediment slug? *Austral Ecology, 33,* 794-806. doi:10.1111/j.1442-9993.2008.01851.x

McCarthy, M. A, Gill, M. A, Lindenmayer, D. B. (1999). Fire regimes in mountain ash forest: evidence from forest age structure, extinction models and wildlife habitat. *Forest Ecology and Management, 124,* 193-203. doi:10.1016/S0378-1127(99)00066-3

McCoy, S. W., Kean, J. W., Coe, J. A., Staley, D. M., Wasklewicz, T.A., & Tucker G. E. (2010). Evolution of a natural debris flow: In situ measurements of flow dynamics, video imagery, and terrestrial laser scanning. *Geology, 38,* 735-738. doi:10.1130/G30928.1

McGuire, L.A., Rengers F. K., Kean J. W., & Staley, D. M. (2017). Debris flow initiation by runoff in a recently burned basin: Is grain-by-grain sediment bulking or en masse failure to blame? *Geophysical Research Letters, 44,* 7310-7319. doi:10.1002/2017GL074243

Meyer, G. A., & Pierce, J. L. (2003). Climatic controls on fire-induced sediment pulses in Yellowstone National Park and central Idaho: a long-term perspective. *Forest Ecology and Management, 178,* 89-104. doi:10.1016/S0378-1127(03)00055-0

Michelini, T., Bettella, F., & D'Agostino, V. (2017). Field investigations of the interaction between debris flows and forest vegetation in two Alpine fans. *Geomorphology, 279,* 150-164. doi:10.1016/j.geomorph.2016.09.029

Montgomery, D. R. (1999). Process domains and the river continuum. JAWRA *Journal of the American Water Resources Association, 35,* 397-410. doi:10.1111/j.1752-1688.1999.tb03598.x

Montgomery, D. R., & Buffington, J. M. (1998). Channel processes, classification, and response. River Ecology and Management. Lessons from the Pacific Coastal Ecoregion. New York: Springer-Verlag: 13-42

Montgomery, D. R., & Foufoula-Georgiou, E. (1993). Channel network source representation using digital elevation models. *Water Resources Research, 29,* 3925 – 3934. doi:10.1029/93WR02463

Moody, J. A. 2017. Residence times and alluvial architecture of a sediment superslug in response to different flow regimes. *Geomorphology, 294,* 40-57. doi:j.geomorph.2017.04.012

Moody, J. A, & Martin, D. A. (2001). Initial hydrologic and geomorphic response following a wildfire in the Colorado Front Range. *Earth Surface Processes and Landforms, 26,* 1049-1070. doi:10.1002/esp.253

Murphy, B. P., Czuba, J. A., and Belmont, P. (2019). Post-wildfire sediment cascades: A modeling framework linking debris flow generation and network-scale sediment routing. *Earth Surface Processes and Landforms*, 44, 2126– 2140. doi:10.1002/esp.4635.

Murphy, S. F., McCleskey, R. B., Martin, D. A., Writer, J. H., & Ebel, B. A. (2018). Fire, Flood, and Drought: Extreme Climate Events Alter Flow Paths and Stream Chemistry. *Journal of Geophysical Research: Biogeosciences, 123,* 2513-2526. doi: 10.1029/2017jg004349

Newton, T., & Rossato, J. (2013). Incident response to 2013 Harrietville bushfires. In *76th Annual Victorian Water Industry Operations Conference & Exhibition*, Bendigo, Australia

Noske. P. J., Nyman, P., Lane, P. N. J., & Sheridan, G. J. (2016). Effects of aridity in controlling the magnitude of runoff and erosion after wildfire. *Water Resources Research, 52,* 4338-4357. doi:10.1002/2015wr017611

Nyman P. (2013). Post-fire debris flows in southeast Australia: initiation, magnitude and landscape controls. (Doctoral dissertation). Retrieved from Minerva Acces (http://hdl.handle.net/11343/38350)

Nyman, P., Smith, H. G., Sherwin, C. B., Langhans, C., Lane P. N. J., & Sheridan, G.J. (2015). Predicting sediment delivery from debris flows after wildfire. *Geomorphology, 250,* 173-186. doi:10.1016/j.geomorph.2015.08.023

Parsons, A. J., Bracken, L., Poeppl, R. E., Wainwright, J., & Keesstra, S. D. (2015). Introduction to special issue on connectivity in water and sediment dynamics. *Earth Surface Processes and Landforms 40,* 1275-1277. doi: 10.1002/esp.3714.

Pelletier, J. D., & Orem, C. A. (2014). How do sediment yields from post-wildfire debris-laden flows depend on terrain slope, soil burn severity class, and drainage basin area? Insights from airborne-LiDAR change detection. *Earth Surface Processes and Landforms, 39,* 1822 -1832, doi:10.1002/esp.3570

Pierce, J. L., Meyer, G. A., & Rittenour, T. (2011). The relation of Holocene fluvial terraces to changes in climate and sediment supply, South Fork Payette River, Idaho. *Quaternary Science Reviews, 30,* 628-645. doi:10.1016/j.quascirev.2010.11.013

Pierson, T.C. (2005). Hyperconcentrated flow — transitional process between water flow and debris flow. Debris-flow Hazards and Related Phenomena. Springer Praxis Books. Springer, Berlin, Heidelberg

Reneau, S. L., Katzman, D., Kuyumjian, G.A., Lavine, A., & Malmon, D. V. (2007). Sediment delivery after a wildfire. *Geology, 35,* 151-154. doi:10.1130/G23288A.1

Rengers, F.K, McGuire, L. A., Kean, J.W., Staley, D.M., & Hobley, D. (2016). Model simulations of flood and debris flow timing in steep catchments after wildfire. *Water Resources Research, 52,* 6041-6061. doi: 10.1002/2015WR018176

Riley, K.L., Bendick, R., Hyde, K. D., & Gabet, E. J. (2013). Frequency–magnitude distribution of debris flows compiled from global data, and comparison with post-fire debris flows in the western US. *Geomorphology, 191,* 118-128. doi:10.1016/j.geomorph.2013.03.008

Roghair, C. N., Dolloff, C. A., & Underwood, M. K. (2002). Response of a Brook Trout Population and Instream Habitat to a Catastrophic Flood and Debris Flow. *Transactions of the American Fisheries Society, 131,* 718-730. doi:10.1577/1548-8659(2002)131<0718:Roabtp>2.0.Co;2

Santi, P. M, deWolfe, V. G, Higgins, J. D, Cannon, S. H., & Gartner, J. E. (2008). Sources of debris flow material in burned areas. *Geomorphology, 96,* 310-321.doi:10.1016/j.geomorph.2007.02.022

Sheridan, G.J., Nyman, P., Langhans, C., Cawson, J., Noske. P. J., Oono, A., Van der Sant, R., & Lane, P. N.J. (2016). Is aridity a high-order control on the hydro–geomorphic response of burned landscapes? *International Journal of Wildland Fire, 25,* 262-267. doi:10.1071/WF14079

Smith, H. G, Sheridan, G. J, Lane, P. N. J., & Bren, L. J. (2011). Wildfire and salvage harvesting effects on runoff generation and sediment exports from radiata pine and eucalypt forest catchments, south-eastern Australia. *Forest Ecology and Management, 261,* 570-581. doi:10.1016/j.foreco.2010.11.009

Smith, H. G., Sheridan, G. J., Lane, P. N. J., Nyman, P., & Haydon, S. (2011). Wildfire effects on water quality in forest catchments: A review with implications for water supply. *Journal of Hydrology, 396,* 170-192. doi:10.1016/j.jhydrol.2010.10.043

Smith, H. G., Sheridan, G. J., Nyman, P., Child, D. P., Lane, P. N. J., Hotchkis, M. A. C., & Jacobsen, G. E. (2012). Quantifying sources of fine sediment supplied to post-fire debris flows using fallout radionuclide tracers. *Geomorphology, 139–140,* 403-415. doi:10.1016/j.geomorph.2011.11.005

Staley, D. M., Negri, J. A,, Kean, J. W., Laber, J. L., Tillery, A. C., & Youberg, A. M. (2017). Prediction of spatially explicit rainfall intensity–duration thresholds for post-fire debris-flow generation in the western United States. *Geomorphology, 278,* 149-162. doi:10.1016/j.geomorph.2016.10.019

Staley, D. M., Tillery, A. C., Kean, J. W., McGuire, L.A., Pauling, H. E., Rengers, F. K., & Smith, J. B. (2018). Estimating post-fire debris-flow hazards prior to wildfire using a statistical analysis of historical distributions of fire severity from remote sensing data. *International Journal of Wildland Fire, 27,* 595 - 608. doi: https://doi.org/10.1071/WF17122

Staley, D. M., Wasklewicz, T. A., & Blaszczynski, J. S. (2006). Surficial patterns of debris flow deposition on alluvial fans in Death Valley, CA using airborne laser swath mapping data. *Geomorphology, 74,* 152-163. doi:10.1016/j.geomorph.2005.07.014

Staley, D. M., Wasklewicz, T. A., & Kean, J. W. (2014). Characterizing the primary material sources and dominant erosional processes for post-fire debris-flow initiation in a headwater basin using multi-temporal terrestrial laser scanning data. *Geomorphology, 214,* 324-338. doi:10.1016/j.geomorph.2014.02.015

Stock, J., & Dietrich, W. E. 2003. Valley incision by debris flows: Evidence of a topographic signature. *Water Resources Research, 39,* 1089. doi:10.1029/2001WR001057

Tomkins, K. M., Humphreys, G. S., Wilkinson, M. T., Fink, D., Hesse, P.P., Doerr, S.H., Shakesby, R. A., Wallbrink, P. J., & Blake, W. H. (2007). Contemporary versus long-term denudation along a passive plate margin: the role of extreme events. *Earth Surface Processes and Landforms, 32,* 1013-1031. doi:10.1002/esp.1460

Tucker, G. E., & Bras, R. L. (1998). Hillslope processes, drainage density, and landscape morphology. *Water Resources Research, 34,* 2751-2764. doi:10.1029/98wr01474

Tucker, G. E., & Hancock, G. R. (2010). Modelling landscape evolution. *Earth Surface Processes and Landforms, 35,* 28-50. doi:10.1002/esp.1952

Van der Sant, R. E. , Nyman, P., Noske, P. J., Langhans, C., Lane, P. N .J, & Sheridan, G. J. (2018). Quantifying relations between surface runoff and aridity after wildfire. *Earth Surface Processes and Landforms, 43,* 2033-2044. doi:10.1002/esp.4370

Whipple, K. X., & Dunne, T. (1992). The influence of debris-flow rheology on fan morphology, Owens Valley, California. *Geological Society of America Bulletin, 104,* 887-900. doi:10.1130/0016-7606(1992)104<0887:TIODFR>2.3.CO;2

Wohl, E. (2017(. Connectivity in rivers. *Progress in Physical Geography, 41*, 345-362. doi:10.1177/0309133317714972

Wolman, M. G. (1954). A method of sampling coarse river-bed material. *Eos, Transactions American Geophysical Union, 35*, 951-956. doi:10.1029/TR035i006p00951

Wondzell, S. M., & King, J. G. 2003. Postfire erosional processes in the Pacific Northwest and Rocky Mountain regions. *Forest Ecology and Management, 178*, 75-87. doi:10.1016/S0378-1127(03)00054-9

Worthy, M., & Wasson, R. (2004). Fire as an agent of geomorphic change in southeastern Australia: implications for water quality in the Australian Capital Territory. In *Regolith*, Roach IC (ed). CRC Landscape Environments and Mineral Exploration: Canberra; 417-418.

Tables

Table 1: Grain size distribution in source areas, taken from data collected in a nearby catchment at Germantown in same geological formation as Washington Creek catchment.

Proportion	< 30 mm	< 2 mm	< 0.2 mm	< 0.02 mm	< 0.002 mm
Hillslope sources	0.96	0.32	0.28	0.16	0.05
Channel sources	0.58	0.32	0.26	0.16	0.06

Table 2: Showing the location of the deposits along the drainage area (*A*), local slope of the arterial channel (*S*), deposit volume (*V*), average deposit width (D_w), channel reach sinuosity (SI), class (DF/HCF), particle size statistics (median, mean, sorting, skewness, and kurtosis) and particle size fractions by volume (Clay & Silts, Sand & Gravel, Pebbles & Cobbles) of the major deposits located in the arterial channel network.

Deposit	Drainage area	Local slope	Volume	Average width	Sinuosity	Class	Particle size statistics			Particle size fractions by volume		
	(*A*)	(*S*)	(*V*)	(D_w)	(SI)	(DF/ HCF)	Median d_{50}	Sorting	Mean	Clay & Silt	Sand & Gravel	Pebbles & Cobbles
	(km^2)	($m\ m^{-1}$)	(m^3)	(m)	(-)		(mm)	(ϕ)	(ϕ)	(%)	(%)	(%)
1	13.8	0.10	597	29.6	1.54	HCF	7.8	1.5	-2.53	0.8	15.6	83.6
2	13.8	0.06	1172	29.6	1.54	HCF	5.4	2.2	-2.88	1.3	18.5	80.2
3	13.7	0.07	286	21.5	1.54	HCF	7.0	1.5	-2.35	0.6	19.0	80.4
4	13.6	0.02	52	14.9	1.54	HCF	6.6	1.3	-2.27	0.6	19.5	79.9
5	13.5	0.09	1512	34.7	1.26	DF	8.5	1.7	-2.85	1.0	10.4	88.6
6	12.9	0.09	298	13.8	1.26	HCF	7.6	1.6	-2.61	1.0	15.1	83.9
7	12.6	0.03	601	16.9	1.28	DF	6.1	1.9	-2.87	0.4	13.8	85.8
8	11.9	0.08	62	11.1	1.28	DF	7.1	1.5	-2.53	1.3	17.1	81.6
9	9.5	0.02	112	12.5	1.16	DF	7.5	1.5	-2.63	0.4	13.4	86.2
10	9.3	0.02	90	19.9	1.16	HCF	6.4	2.0	-2.83	0.3	13.9	85.7
11	9.3	0.11	1573	24.5	1.16	DF	13.2	2.2	-3.63	0.2	6.3	93.5
12	4.2	0.10	1190	18.5	1.28	DF	6.5	1.7	-2.57	0.9	17.2	81.9
13	4.2	0.13	732	26.8	1.41	DF	12.6	1.3	-4.03	0.1	1.6	98.2
14	2.0	0.21	517	24.4	1.41	DF	8.3	1.4	-2.61	1.5	12.7	85.9
15	1.9	0.31	218	14.6	1.41	DF	7.3	1.4	-2.45	1.7	16.9	81.4
16	1.8	0.25	111	21.3	1.10	DF	11.0	1.2	-3.56	0.1	3.2	96.7
17	1.5	0.13	287	19.1	1.10	DF	6.5	1.6	-2.32	3.1	17.8	79.1
18	0.7	0.16	185	22.1	1.10	DF	7.2	1.2	-2.32	3.2	15.7	81.1
19	2.1	0.24	83	17.5	1.15	DF	9.6	2.0	-3.55	0.4	6.5	93.1
20	1.8	0.14	288	21.7	1.15	DF	10.9	2.0	-3.38	0.5	7.7	91.8
21	1.5	0.19	314	21.3	1.10	DF	8.9	1.6	-3.10	1.2	7.5	91.3
22	1.2	0.24	694	22.4	1.10	DF	10.0	2.3	-3.26	0.7	9.4	89.9
23	4.9	0.09	27	13.2	1.26	DF	17.4	1.9	-3.62	0.1	3.2	96.7
24	4.3	0.09	84	12.4	1.26	HCF	9.4	1.9	-3.05	0.3	8.8	90.9
25	3.4	0.11	237	13.9	1.15	DF	15.1	1.9	-4.35	0.1	2.4	97.6
26	2.0	0.11	150	15.3	1.151	HCF	8.4	1.7	-2.89	0.9	11.3	87.8
27	1.9	0.18	1303	23.1	1.15	DF	7.4	1.4	-2.38	1.5	16.9	81.6

Figure captions

Figure 1. Map showing the topography, drainage network (channels of stream order ≥ 4) and type of burn in the Upper Ovens catchment in southeast Australia. Washington Creek catchment outlined in dashed black line.

Figure 2. a) Orthorectified aerial imagery (15 cm resolution) of Washington Creek showing location debris-flow source areas (borders coloured light blue), and the 27 major deposits (red arrows) that were measured with cross-sections during the field campaigns. The source areas were defined as the 1-3rd stream order tributary channels that produced debris flows. b) Schematic top view and cross-sectional view of a deposit and the method used to calculate its volume.

Figure 3. a) Deposit volume, V (m^3), plotted in relation to drainage area, A (m^2), and local slope, S (m m^{-1}). The mean of slope-area data showing together with curve fitted from Stock and Dietrich (2003: Equation 5). The size of the bubbles is proportional to the volume of deposition (m^3). b) Sorting (σ_ϕ) and median particle size, d_{50}, with drainage area. c) The coefficient of fixation (d_{50}/S) with A. d): The volumetric fraction of clay and silts (d < 0.063 mm), sand (0.063≤ d< 2 mm) and pebbles and cobbles (d ≥ 2 mm) of the deposits.

Figure 4: Volumetric grain size distribution of deposits classified into debris flow (DF) and hyperconcentrated flow (HCF). The mean grain size distribution of the 20 DF (red coloured) and 7 HCF (blue coloured) deposits is shown by the solid lines. Standard deviations are drawn as vertical bars. The grain size distribution for hillslope and channels (1-3rd order streams) from a nearby catchment at Germantown (from Nyman, 2013) is shown for comparison.

Figure 5. Maps of erosion, deposition and accumulated volumes in Washington Creek. Erosion and deposition are shown in units of m^3 per grid cell in the 10m DEM. Volume is the sum of net erosion along the direction of flow. The mapped debris-flow source areas are outlined with grey lines. a) Modelled erosion volumes. b) Combined modelled and measured

deposition. Estimated from field measurements in the arterial channel and modelled in source areas. c) Net erosion obtained from a) and b). d) Sediment volume in obtained by accumulating net erosion along the direction of flow according to a D8 flow routing algorithm.

Figure 6: Sediment budget showing deposition and erosion volumes (units are in x 10^3 m^3) in in different geomorphic units in the Washington Creek catchment. Methods for estimating uncertainty are shown in Supporting Information (Equations S1 - S8)

Figure 7. A debris flow from a 1^{st} stream order channel spilling into a 5^{th} stream order channel of the Washington Creek catchment. The role of reworking by water for transport of fines indicated by differences in colour of the in-channel sediment (pale) and intact parts of the debris-flow fan (reddish brown).

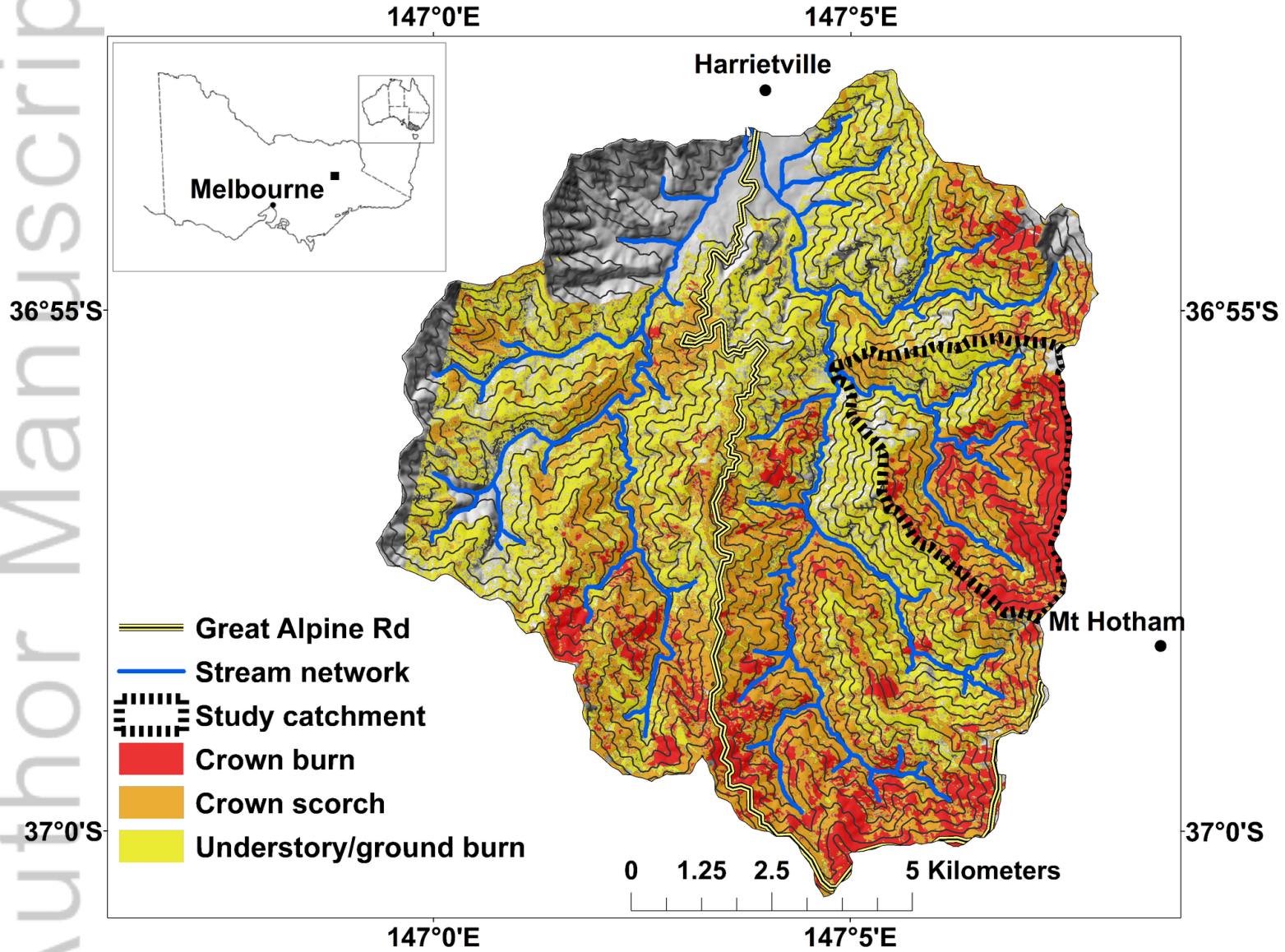

ESP_4785_Figure1.tiff

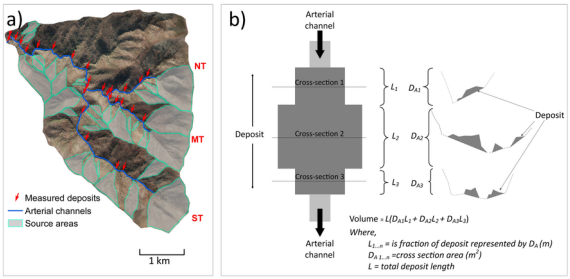

ESP_4785_Figure2.tif

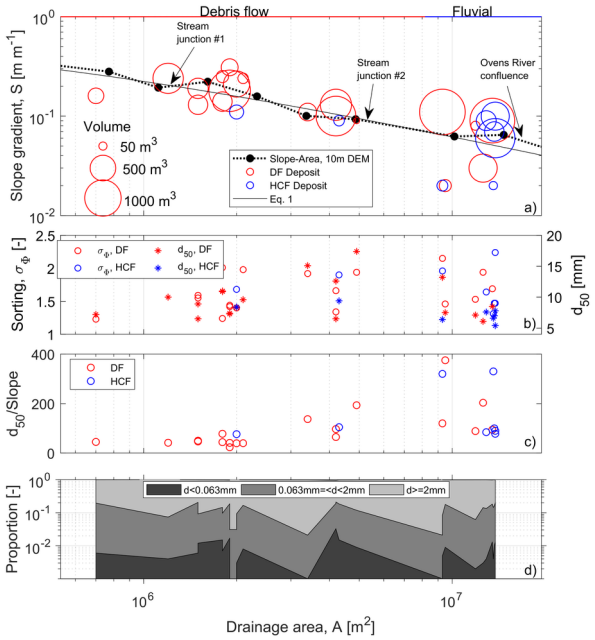

ESP_4785_Figure3.tif

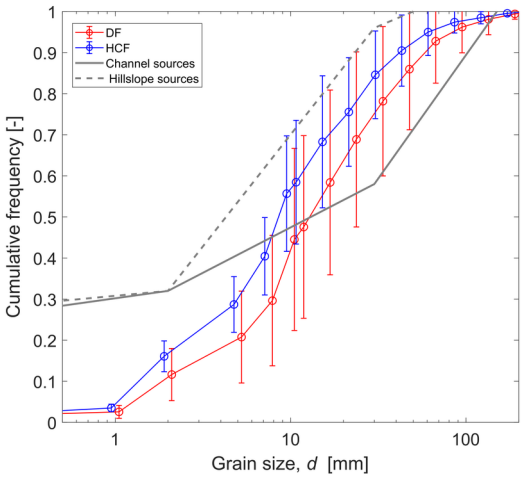

ESP_4785_Figure4.tif

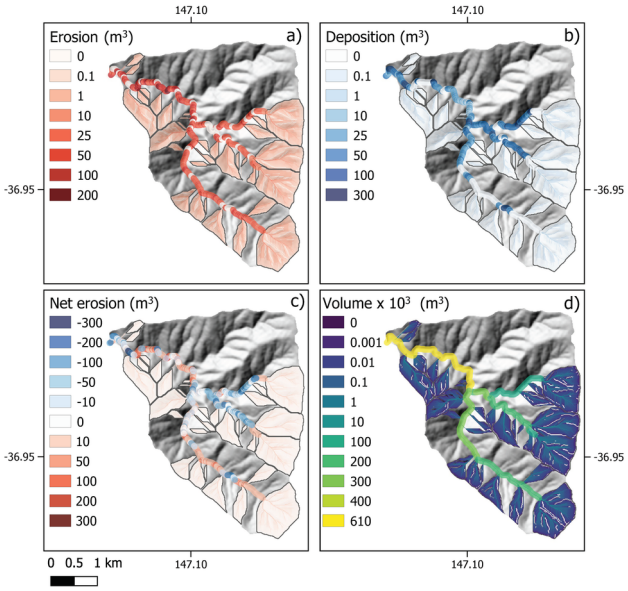

ESP_4785_Figure5.tif

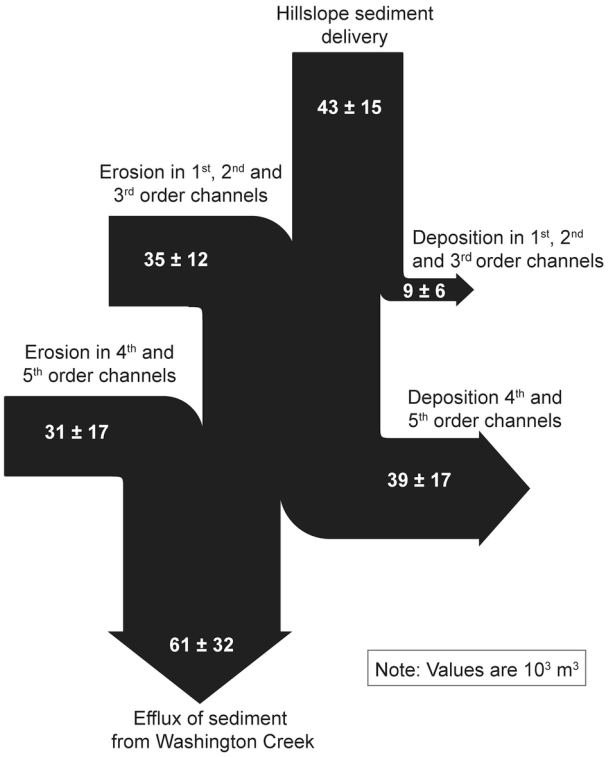

ESP_4785_Figure6.tiff

ESP_4785_Figure7.jpg